Journal Pre-proofs

Benzopyrimidodiazepinone inhibitors of TNK2

Brian J. Groendyke, Chelsea E. Powell, Frederic Feru, Thomas W. Gero, Zhengnian Li, Hilary Szabo, Kevin Pang, John Feutrill, Bailing Chen, Bin Li, Nathanael S. Gray, David A. Scott

PII: S0960-894X(20)30001-9
DOI: https://doi.org/10.1016/j.bmcl.2020.126948
Reference: BMCL 126948

To appear in: *Bioorganic & Medicinal Chemistry Letters*

Received Date: 19 November 2019
Revised Date: 20 December 2019
Accepted Date: 1 January 2020

Please cite this article as: Groendyke, B.J., Powell, C.E., Feru, F., Gero, T.W., Li, Z., Szabo, H., Pang, K., Feutrill, J., Chen, B., Li, B., Gray, N.S., Scott, D.A., Benzopyrimidodiazepinone inhibitors of TNK2, *Bioorganic & Medicinal Chemistry Letters* (2020), doi: https://doi.org/10.1016/j.bmcl.2020.126948

Bioorganic & Medicinal Chemistry Letters
journal homepage: www.elsevier.com

Benzopyrimidodiazepinone inhibitors of TNK2

Brian J. Groendyke[a,b], Chelsea E. Powell[a,b], Frederic Feru[a,b], Thomas W. Gero[a,b], Zhengnian Li[a,b], Hilary Szabo[c], Kevin Pang[d], John Feutrill[e], Bailing Chen[e], Bin Li[e], Nathanael S. Gray[a,b], David A. Scott*[,a,b]

[a] *Department of Cancer Biology, Dana-Farber Cancer Institute, Boston, MA 02115, USA.*
[b] *Department of Biological Chemistry & Molecular Pharmacology, Harvard Medical School, 360 Longwood Ave, Boston, MA 02115, USA.*
c Vivid BioSciences, 50 Northern Ave, Boston, MA 02210, USA
d Northeastern University, 360 Huntington Ave, Boston, MA 02115, USA.
e SYNthesis med chem, 425 Changyang Street, Suzhou Industry Park, Suzhou, Jiangsu, China.

ARTICLE INFO

Article history:
Received
Revised
Accepted
Available online

Keywords:
TNK2
Kinase inhibitor
Benzopyrimidodiazepinone

ABSTRACT

The SAR of a series of benzopyrimidodiazepinone inhibitors of TNK2 was developed, starting from the potent and selective compound XMD8-87. A diverse set of anilines was introduced in an effort to improve the *in vivo* PK profile and minimize the risk of quinone diimine formation.

a cytoplasmic kinase that was first identified based on its binding to cell division control protein 42 homolog (CDC42), a cell-cycle regulator.[1] TNK2 acts as an effector of CDC42, which in turn regulates cell migration.[2] Over-expression of TNK2 in cancer cell lines can increase cellular motility, invasiveness, and the ability of cells to metastasize.[3] TNK2 mutations and/or over-expression are associated with numerous cancers, including renal, lung, ovarian, gastric, prostate, and breast cancers.[4] Small molecule inhibitors of TNK2 from several structural classes have been explored as potential treatments for some of these indications, though none have yet reached the clinic.[5-8] Recently, Maxson et al. identified two point mutations, D163E and R806Q, in TNK2 that act as driver mutations of acute myelogenous leukemia (AML) suggesting that TNK2 inhibitors may have utility as a therapy for AML.[4]

The tricyclic benzopyrimidodiazepinone series and related scaffolds have delivered both highly selective tool compounds,[4, 9-11] and advanced lead molecules for ERK5, (XMD8-92)[12,13] and LRRK2, (LRRK2-IN-1)[14] (Fig 1). Most compounds derived from this scaffold have an aniline group installed on the pyrimidine ring, and for these inhibitors the overall kinase selectivity profile is often enhanced by a methoxy substituent at the aniline 2-position. The 2-MeO aniline group is present in other pyrimidine-based kinase inhibitor scaffolds,[15-18] but is not sufficient by itself to confer good selectivity. The high degree of overall kinase selectivity achievable in the benzopyrimidodiazepinone series is likely to be driven by the combination of the 2-MeO aniline and the tricyclic core, with additional substituents on the core and the aniline.

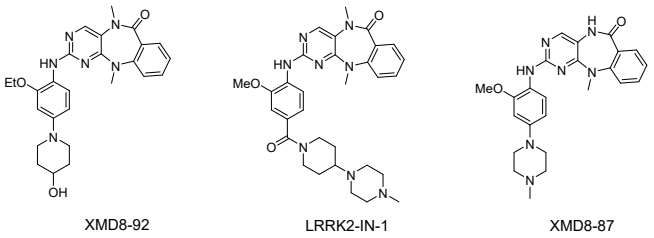

Figure 1. Benzopyrimidodiazepinone kinase inhibitors

Kinase selectivity profiling of multiple examples from the benzopyrimidodiazepinone series led to the identification of XMD8-87 as a potent and highly selective TNK2 inhibitor.[4,19] XMD8-87 showed little activity against other kinases in both the Kinativ[20] and KinomeScan[21] panels (SI – Fig 1) of 241 and 402 kinases respectively and is a useful pharmacological tool to explore the effects of TNK2 inhibition. Based on our kinase profiling data, benzopyrimidodiazepinones unsubstituted on the central ring amide showed the greatest activity against TNK2. In our work targeting other kinases with this series, we typically observed increased potency for compounds with a methyl substituent on the amide. For TNK2, modeling studies suggested that the amide NH interacts with the Thr205 gatekeeper residue, in a manner similar to that reported for a co-crystal structure with TNK2 and an aminopyrazolopyrimidine.[6]

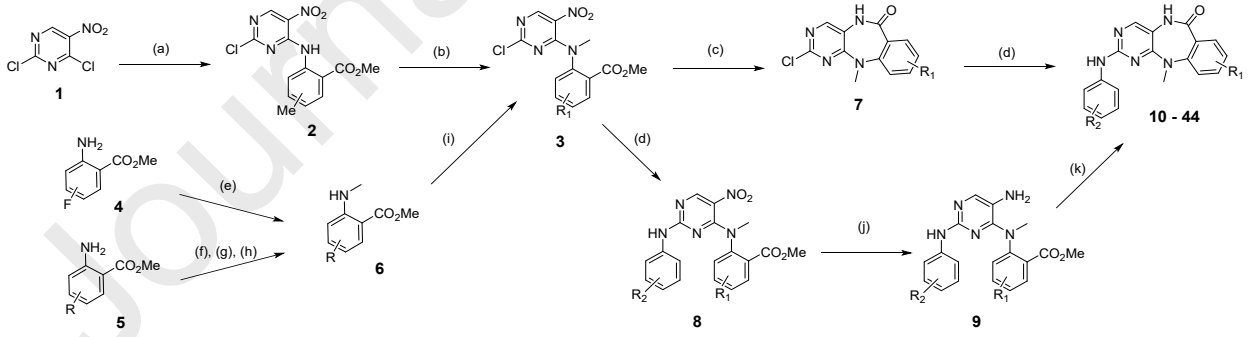

Scheme 1. Synthesis of benzopyrimidodiazepinones. Reagents and conditions: (a) methyl anthranilate, $^{i}Pr_2NEt$, $^{i}PrOH$; (b) NaH, MeI, DMF; (c) Fe, AcOH, 50°C; (d) aniline, $Pd_2(dba)_3$, Xphos, K_2CO_3, $^{t}BuOH$, 100°C; (e) MeI, K_2CO_3, acetone, 65°C; (f) $(CF_3CO)_2O$, $^{i}Pr_2NEt$, DCM; (g) MeI, K_2CO_3, DMF; (h) NaOMe, MeOH; (i) 2,4-dichloro-5-nitropyrimidine, $^{i}Pr_2NEt$, dioxane, 50°C; (j) H_2, Pd/C, MeOH; (k) TsOH, dioxane, MW, 150°C.

Disappointingly, XMD8-87 was very highly cleared *in vivo* in rodent PK studies (Table 4). This was in contrast to several *N*-methyl amide examples designed to target other kinases,[12-14] and also XMD8-85, the *N*-methyl matched pair of XMD8-87, all of which demonstrated good *in vivo* mouse PK profiles.

With the goal of developing a TNK2 inhibitor from the benzopyrimidodiazepinone series, we sought to explore the SAR and improve the *in vivo* PK profile. We introduced substituents to the phenyl ring of the tricyclic core and explored a broader range of anilines and aniline replacements at the C2 position of the pyrimidine ring. We were keen to retain the exquisite kinase selectivity of XMD8-87 to help confirm the relevance of TNK2 as a therapeutic target.

Compounds were prepared using chemistry similar to that previously described (Scheme 1), with modifications to the reaction sequence depending upon starting material availability and differences in intermediate reactivity for some steps.[12] Anthranilic esters were installed at the 4-position of 2,4-dichloro-5-nitropyrimidine, either as the primary anilines to give **2**, with a subsequent methylation step, or as the *N*-methyl anilines, to give **3**. The *N*-methylanilines **6** were commercially available or prepared by methylation of either the primary aniline or trifluoroacetamide. A one-pot reduction/cyclization was achieved with iron in acetic acid and moderate heating for most examples to give the tricyclic core **7**, with a final step to via Pd coupling chemistry. In some cases, the second aniline was incorporated prior to the cyclization step to generate the bisanilinopyrimidines **8**, and a two-step nitro reduction/cyclization sequence was employed to generate the final compounds. Characterization data for the final compounds is included in the Supplementary Data.

TNK2 enzyme IC50s and cell data for compounds with modifications to the phenyl ring are shown in Table 1. None of the substituents we introduced to the phenyl ring led to significantly improved potency in either the TNK2 enzyme assay,[22] or TNK2 D163E cell assay.[23] The majority of compounds showed reduced TNK2 activity relative to XMD8-87 in both the enzyme and cell, but a methyl group adjacent to the central ring amine was tolerated (**13**) and fluorine could be introduced at two positions (**15**, **17**) without much impact on potency. We also profiled XMD8-85, the *N*-methyl amide analog of XMD8-87, and confirmed that the loss of the amide NH led to reduced TNK2 potency in the enzyme and cell assays.

Table 1. Phenyl ring SAR; compounds **10-19**

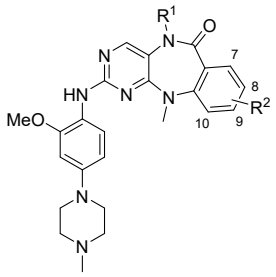

Compound	R^1	R^2	TNK2 IC_{50} (nM)[a]	Cell TNK2 D163E (uM)
XMD8-87	-	-	44	0.19
XMD8-85	Me	-	959	0.56
10	-	7-Me	1610	1.63
11	-	8-Me	363	1.92
12	-	9-Me	223	0.26
13	-	10-Me	73*	0.13
14	-	7-F	217	0.38
15	-	8-F	26*	0.09
16	-	9-F	308	1.01
17	-	10-F	101	0.23
18	-	8-CN	723	3.59
19	-	9-CN	2480	1.39

Table 2. Aniline SAR, 2- and 3-positions; compounds **20-27**

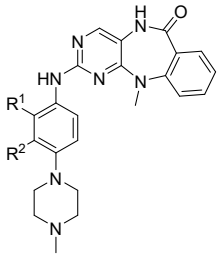

Compound	R^1	R^2	TNK2 IC_{50} (nM)[a]	Cell TNK2 D163E (uM)
XMD8-87	OMe	H	44	0.19
20	H	H	16*	0.04

21				
22	Me	H	97	0.37
23	Cl	H	63	0.38
24	H	OMe	4	0.012
26	H	Me	6	0.05
27	H	Cl	11	0.10

[a] Data was generated at BioDuro or ThermoFisher (*).

We felt that small modifications on the phenyl ring of the tricyclic core were unlikely to significantly impact the PK profile of the series, and therefore focused our efforts on the aniline substituent. We prepared a set of compounds combining small substituents at the aniline 2- and 3-positions with a 4-*N*-methyl piperazine group (Table 2). Compound **20**, lacking the 2-MeO group, was more potent than XMD8-87, but our archive of kinase profiling data (including Kinativ data for **29**)[4] suggested that compounds of this type were less selective. A small substituent at the aniline 3-position led to enhanced TNK2 potency in both enzyme and cells (e.g. **24**) but reduced selectivity in the KinomeScan panel (SI – Figure 1), and we concluded that 2-MeO gave the best balance of potency and kinase selectivity.

We also prepared a set of compounds with structurally diverse cyclic amines at the 4-position, designed to deliver acceptable physical properties (Table 3). The 1,4-diamino substitution pattern on a phenyl ring is a perceived risk in terms of formation of a reactive quinone diimine. This concern has been mitigated previously for kinase inhibitors by replacing a piperazine substituent at the aniline 4-position with a piperidine.[24-26] In addition to compounds such as **28**, **30**, **31** and **32**, we therefore prepared compounds with a carbon-linked piperidine (**33**, **34**). Compounds with the 2-MeO substituent and a piperazine or *N*-linked piperidine at the aniline 4-position typically showed good potency in our cell assay, while the C-linked piperidines (**33**, **34**) were less potent. 3-MeO anilines (**35** - **37**) delivered consistently improved potency in both the enzyme and cell assays, but we assumed that their overall kinase selectivity profiles would resemble that of **24**. Moving the piperazine substituent to the 3-position (**38**) led to a 10-fold reduction in enzyme and cell potency. We also installed bicyclic anilines as an alternative strategy to mitigate potential quinone diimine formation, following the approach adopted in the development of tetrahydroisoquinoline pyrimidine ALK inhibitors.[27] As with the monocyclic aniline examples, compounds without the 2-MeO group (**39**, **41**, **43**) were more potent in the enzyme and cell.

We did not see a good correlation between *in vitro* and *in vivo* PK for this series, with compounds frequently showing good stability in mouse microsomes and hepatocytes. In particular, the *in vitro* data for XMD8-87 and *N*-methyl analog XMD8-85 was similar (Table 4), despite different rates of *in vivo* clearance. The contrasting PK profiles of XMD8-87 and XMD8-85 suggested that the poor PK of the former derived from the tricyclic core rather than the aniline. However, *in vitro* metabolite ID data did not suggest a metabolic pathway that directly involved the unsubstituted amide. Instead, an oxidation step appeared to be the major metabolic pathway for XMD8-87, with the only significant metabolite corresponding to a molecular weight one less than the parent (Table 5 and SI Figure 2). This was also the major metabolite in rat urine in an *in vivo* metabolite ID study, and we speculated that it corresponded to the quinone diimine. The corresponding GSH adduct was observed in rat bile from the same study. The *in vitro* metabolite ID data for the *N*-methyl analog XMD8-85 showed a similar metabolite, but with a reduced rate of conversion (SI Figure 3).

Examples **31-34** were profiled for IV PK in mice, and we observed high levels of clearance, similar to those seen with XMD8-87. This was especially disappointing for the piperidine examples, as an *in vitro* metabolite ID study with **33** showed a reduced rate of conversion to the MW-1 oxidation product (SI Figure 4).

Table 3. Aniline SAR, amines; compounds **28-44**

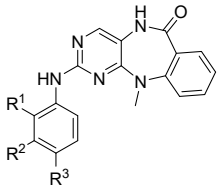

Compound	R^1	R^2	R^3 or aniline replacement	TNK2 IC50 (nM) [a]	Cell TNK2 D163E (uM)
XMD8-87	OMe	H	*N*-Me piperazine	44	0.19
28	OMe	H	4-OH piperidine	37*	0.14
29	H	H	4-OH piperidine	7*	0.08
30	OMe	H	morpholine	41	0.19

31			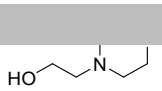			**39**	-	-	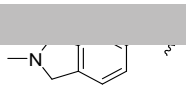	
32	OMe	H	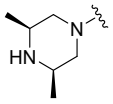	29	0.06	**40**	-	-	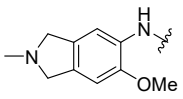	91	0.85
33	OMe	H	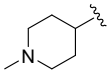	62	0.25	**41**	-	-	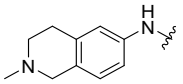	18	0.11
34	OMe	H	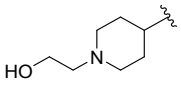	66	0.26	**42**	-	-	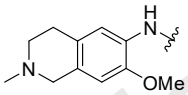	50	0.26
35	H	OMe	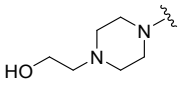	7	0.013	**43**	-	-	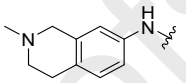	28	0.12
36	H	OMe	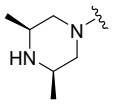	4	0.013	**44**	-	-	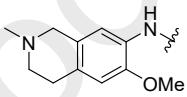	140	0.11
37	H	OMe	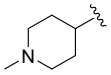	13	0.14						
38	-	-	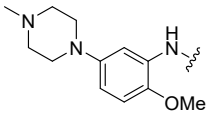	254	1.10						

[a] Data was generated at BioDuro or ThermoFisher (*).

Table 4. Mouse microsome and hepatocyte stability, and *in vivo* mouse PK[a] data (3mpk IV, 10mpk PO)

Compound ID	Mouse microsomes ($T_{1/2}$)	Mouse hepatocytes ($T_{1/2}$)	IV Cl (ml/min/kg)	IV $T_{1/2}$ (hr)	F %	Auc inf (PO) (ng*hr/ml)
XMD8-87	28	347 mins	150	0.7	5	56
XMD8-85	22	>500	25	4.4	46	2000
31	139	75	140	2.0	-	-
32	-	-	130	0.9	11	141
33	94	64	100	1.7	-	-
34	-	-	130	1.8	-	-
42	-	-	120	10	7	125
44	-	-	86	1.4	22	525

[a] PK studies were conducted in male CD-1 mice, and all values are an average from three animals

A series of pyrrolotriazine kinase inhibitors containing a 1,4-diamino substituted aniline were reported to give unusually high levels of GSH adducts via formation of the reactive quinone diimine.[28] This was mitigated by the replacement of the piperazine substituent with a piperidine.[25] The data suggested that relative to other chemical series, the pyrrolotriazine scaffold greatly increased the susceptibility of the 1,4-diamino aniline to oxidation, perhaps through interactions with the P450 active site. Similarly, it is possible that benzopyrimidodiazepinones such as XMD8-87 may be susceptible to much higher rates of oxidation to the quinone diimine than the corresponding methylated scaffold. This could result in greatly increased *in vivo* clearance, although we did not observe a correlation between the rate of metabolite formation in our *in vitro* metabolite ID studies and mouse IV Cl.

In vitro metabolite ID data for examples with a bicyclic aniline **41** and **44** (SI Figure 5) showed a distinct profile relative to the other compounds, suggesting an alternative metabolic pathway. For both compounds, there was no evidence of the MW-1 metabolite, with the main routes of metabolism being conversion to an oxidation product (+16) or demethylation (-14). For **44**, the rate of conversion of the parent appeared relatively slow. Disappointingly, however, the *in vivo* PK data for bicyclic anilines **42** and **44** showed only a limited improvement over XMD8-87, with high IV Cl for both compounds.

In conclusion, we have developed the SAR of the benzopyrimidodiazepinone series in regard to TNK2 inhibition and pursued several approaches to mitigate the unexpectedly high *in vivo* clearance for examples of this scaffold. Our further efforts to optimize this series will be reported in due course.

Table 5. *In vitro* metabolite ID studies in mouse liver microsomes

Compound	Parent (m/z)+	Major metabolite (m/z)+	Other metabolites (m/z)+	Incubation time (mins)
XMD8-87	446.2 (2%)	445.2 (98%)	< 1%	60
XMD8-85	460.3 (40%)	459.3 (53%)	446.2 (6%)	60
33	445.2 (75%)	444.2 (23%)	< 2%	120
41	387.2 (17%)	403.2 (73%)	373.2 (10%)	120
44	417.2 (64%)	433.2 (11%)	403.2 (11%), 415.2 (10%)	120

Acknowledgments

Ba/F3 cells expressing TNK2 D163E were generously provided by Jeffrey W. Tyner (Oregon Health and Science University, Portland, OR). *In vitro* and *in vivo* PK studies were conducted at BioDuro, Shanghai, under the supervision of Cindy Liang and Ying Zhou. We thank Vivid BioSciences for funding support.

References and notes

1. Manser, E.; Leung, T.; Salihuddin, H. et al. *Nature*, **1993**, *363*, 364.
2. Modzelewska, K.; Newman, L. P.; Desai, R.; Keely, P. J. *J Biol Chem.* **2006**, *281*, 37527.
3. van der Horst, E. H.; Degenhardt, Y. Y.; Strelow, A. et al. *Proc Natl Acad Sci USA*. **2005**, *102*, 15901.
4. Maxson, J. E.; Abel, M. L.; Wang, J. et al. *Cancer Res*. **2016**, *76*, 127.
5. Jin, M.; Wang, J.; Kleinberg, A. et al. *Bioorg Med Chem Lett.* **2013**, *23*, 979.
6. Kopecky, D. J.; Hao, X.; Chen, Y. et al. *Bioorg Med Chem Lett.* **2008**, *18*, 6352.
7. Jiao, X.; Kopecky, D. J.; Liu, J. et al. *Bioorg Med Chem Lett.* **2012**, *22*, 6212.
8. Lawrence, H. R.; Mahajan, K.; Luo, Y. et al. *J Med Chem*. **2015**, *58*, 2746.
9. Fan, F.; He, Z.; Kong, L. L. et al. *Sci Transl Med*. **2016**, *8*, 352ra108.
10. Ferguson, F. M.; Ni, J.; Zhang, T. et al. *ACS Med Chem Lett*. **2016**, *7*, 908.
11. Banerjee, S.; Buhrlage, S. J.; Huang, H. T. et al. *Biochem J.* **2014**, *457*, 215.
12. Deng, X.; Yang, Q.; Kwiatkowski, N. et al. *ACS Med Chem Lett.* **2011**, *2*, 195.
13. Deng, X.; Elkins, J. M.; Zhang, J. et al. *Eur J Med Chem.* **2013**, *70*, 758.
14. Deng, X.; Dzamko, N.; Prescott, A. et al. *Nat Chem Biol.* **2011**, *7*, 203.

57, 8249.
16. Galkin, A. V.; Melnick, J. S.; Kim, S. et al. *Proc Natl Acad Sci USA*. **2007**, *104*, 270.
17. Huang, W. S.; Liu, S.; Zou, D. et al. *J Med Chem.* **2016**, *59*, 4948.
18. Rudolph, D.; Steegmaier, M.; Hoffmann, M. et al *Clin Cancer Res.* **2009**, *15*, 3094.
19. Miduturu, C. V.; Deng, X.; Kwiatkowski, N. et al *Chem Biol*. **2011**, *18*, 868.
20. Patricelli, M. P.; Szardenings, A. K.; Liyanage, M. et al. *Biochemistry.* **2007**, *46*, 350.
21. Davis, M. I.; Hunt, J. P.; Herrgard, S. et al. *Nat Biotechnol.* **2011**, *29*, 1046.
22. Enzyme testing was conducted at BioDuro or at ThermoFisher, using an HTRF LanthaScreen assay. For compounds tested at both sites, there was an excellent correlation between the two assays, with the ThermoFisher assay typically showing slightly increased sensitivity (compounds up to 2-fold more potent).
23. We used a cell viability assay based on Ba/F3 cells expressing TNK2 D163E. Cells were plated at a volume of 50 µL with a density of 105 cells/mL in white 384-well plates (Corning 3570). 100 nL of compound in DMSO from stock plates was added by pin transfer using a Janus Workstation (PerkinElmer). After 72 hr, cell viability was evaluated using the CellTiter-Glo Luminescent Cell Viability Assay (Promega) following the manufacturer's standards. IC50s were modeled from 3 biological replicates using GraphPad Prism 8 software.
24. Marsilje, T. H.; Pei, W.; Chen, B. et al. *J Med Chem.* **2013**, *56*, 5675.
25. Mesaros, E. F.; Thieu, T. V.; Wells, G. J. et al. *J Med Chem.* **2012**, *55*, 115.
26. Weinberg, L. R.; Albom, M. S.; Angeles, T. S. et al. *Bioorg Med Chem Lett.* **2011**, *21*, 7325.
27. Achary, R.; Yun, J. I.; Park, C. M. et al. *Bioorg Med Chem*. **2016**, *24*, 207.
28. Wells-Knecht, K. J.; Ott, G. R. Cheng, M. et al. *Chem Res Toxicol.* **2011**, *24*, 1994.

Supplementary Material

Declaration of interests

X The authors declare that they have no known competing financial interests or personal relationships that could have appeared to influence the work reported in this paper.

☐The authors declare the following financial interests/personal relationships which may be considered as potential competing interests:

Graphical Abstract

To create your abstract, type over the instructions in the template box below.
Fonts or abstract dimensions

Benzopyrimidodiazepinone inhibitors of TNK2

Leave this area blank for abstract info.

Brian J. Groendyke, Chelsea E. Powell, Frederic Feru, Thomas W. Gero, Zhengnian Li, Hilary Szabo, Kevin Pang, John Feutrill, Bailing Chen, Bin Li, Nathanael S. Gray, David A. Scott